Materials Research Proceedings 41 (2024) 1038-1047 https://doi.org/10.21741/9781644903131-114

Characterization of the superplastic behavior of a Ti6Al4V-ELI alloy bilayer sheet

GUGLIELMI Pasquale[1,a *], PICCININNI Antonio[1,b], CUSANNO Angela[1,c], VAIANI Lorenzo[1,d], UVA Antonio Emmanuele[1,e], PALUMBO Gianfranco[1,f]

[1]DMMM - Politecnico di Bari, Viale Japigia 182, Bari 70126, Italy

[a]pasquale.guglielmi@poliba.it, [b]antonio.piccininni@poliba.it, [c]angela.cusanno@poliba.it, [d]lorenzo.vaiani@poliba.it, [e]antonio.uva@poliba.it, [f]gianfranco.palumbo@poliba.it

Keywords: Ti Alloy, Material Characterization, Superplasticity, Finite Element, Inverse Analysis

Abstract. The aim of the present work is to investigate the superplastic behaviour of a bilayer Ti6Al4V-ELI to numerically design a full custom prosthesis manufacturing process by means of SuperPlastic Forming (SPF); the bilayer was composed by: (i) a monolithic Titanium blank (cut by a rolled sheet); (b) a porous blank cut by a billet produced by Hot Isostatic Pressing (HIP) and subjected to a Solid State Foaming (SSF) heat treatment. Experimental bulge tests aimed to evaluate the effects of both the initial porosity level of the HIPed layer and the temperature (850 and 900 °C) of the SPF process. The bilayer sample was deformed by a constant argon gas pressure and the time evolution of the dome height was recorded during the test in order to be used as target in the IA to determine the constants of the rheological model of the porous layer, being the behavior of the monolithic layer already known. A 2D FE model of the free inflation test was integrated in an automatic optimization procedure with the aim to minimize the error between the calculated and the acquired dome height vs time curve. Finally, the obtained material constants determined were used to design the SPF process by means of the numerical simulation, identifying as a case study a zygomatic full custom prosthesis. The initial porosity level resulted to poorly affect the superplastic behavior of the bilayer at 850 °C; on the contrary, when increasing the temperature up to 900 °C, an evident reduction of the forming time was obtained. Numerical simulations showed that at 900 °C it is possible to obtain the very complex geometry of the adopted case study in about 50000 seconds.

Introduction

Titanium (Ti) alloys are characterized by a wide range of applications because of their physical and chemical properties. High corrosion resistance properties and high strength combined with weight savings are highly valued by the chemistry and aerospace industries. In recent years, these properties together with biocompatibility with body fluids have motivated their adoption in the biomedical field for manufacturing prosthetic implants. In this regard, one of the most important aspects is the durability of the implant without any infectious risk to the host patient. Not surprisingly, large differences in terms of Young's modulus between the human bone and the prosthesis material cause stress-shielding phenomena. To avoid this problem, one possible solution is the adoption of porous structures capable of modifying the elastic response; the presence of porous structures also promotes bone tissue regeneration. In fact, porous-structure materials are increasingly used because of their attractive physical and mechanical properties, such as high specific strength directly related to the amount and size of pores. In addition, when optimally designed, they are characterized by a significant increase in energy dissipation and vibration absorption capacity, not disdaining appreciable thermal as well as acoustic properties. According to this, one possible solution is to adopt Ti alloys obtained by Hot Isostatic Pressing (HIP) [1] subsequently subjected to a Solid State Foaming (SSF) heat treatment [2] aimed at changing the

porosity level [3]. In addition, the growing demand for fully customized prostheses has increased the geometric complexity of the implants. Among others, SPF could be an appropriate choice to ensure complex shapes [4]. The correct process design requires a reliable Finite Element (FE) model, based on an accurate material modelling. In addition to the economic savings due to the reduction of the experiments, thanks to the possibility of coupling a numerical model to an optimization loop, the adoption of the numerical modeling represents an increasingly more essential solution. Regarding the SPF process, the FE method is usually adopted to predict both the final thickness distribution and the optimal pressure profile. In this regard, a robust characterization of the material is necessary [5]. To this should also be added the significant role of the type of material model adopted to reproduce in the FE environment the mechanical and deformation properties of the material. To confirm this, several research activities are based on this objective. According to the evidence obtained by Enikeev and Kruglov [6], it is possible to determine the constants of the material model exclusively by means of bulge tests. In order to reduce as much as possible, the number of experimental tests required for the material characterization, a highly valuable tool is represented by IA [7]. The IA aims at the determination of the objective function(s) through the minimization of the error between the experimental data and that of the prediction model.

The present work aims at investigating the superplastic behaviour of a bilayer Ti6Al4V-ELI to numerically design a full custom prosthesis manufacturing process by means of SuperPlastic Forming (SPF); the bilayer was composed by: (i) a monolithic Titanium blank (cut by a rolled sheet); (b) a porous blank cut by a billet produced by Hot Isostatic Pressing (HIP) and subjected to a Solid State Foaming (SSF) heat treatment. Experimental bulge tests aimed to evaluate the effects of both the initial porosity level of the HIPed layer and the temperature (850 and 900 °C) of the SPF process. The bilayer sample was deformed by a constant argon gas pressure and the time evolution of the dome height was recorded during the test in order to be used as target in the IA to determine the constants of the rheological model of the porous layer, being the behavior of the monolithic layer already known. A 2D FE model of the free inflation test was integrated in an automatic optimization procedure with the aim to minimize the error between the calculated and the acquired dome height vs time curve. Finally, the obtained material constants determined were used to design the SPF process by means of the numerical simulation, identifying as a case study a zygomatic full custom prosthesis.

Material and Methods

The experimental campaign aimed to evaluate the effectiveness of this approach to reduce the final component production time without disdaining the mechanical and functional performance of the final component. Unfortunately, as demonstrated in a previous work [8], it is not possible to characterize under superplastic conditions individually the HIPed layer because of the coalescence of porosities resulting in gas leakage during the test, which makes the blank deformation not possible. Based on this, experimental tests were performed directly on the bilayer by placing the monolithic blank in direct contact with Argon gas. Then, by implementing the data in the AI, it was possible to obtain the HIPed material's constants under superplastic conditions, considering also the constants referred to the BULK layer determined separately. Finally, the obtained values were implemented in a FE numerical model to design a hybrid full custom prosthesis.

Material

The experimental activity was conducted using a 2 layers titanium blank obtained by rolling (named BULK) and by HIP process. Regarding the HIPed material, the manufacturing process was characterized by (i) Argon pressure of 0.2 MPa and (ii) HIP pressure equal to 80 MPa. Ti6Al4V-ELI powders with a diameter ranging from 50 to 100 μm were used. From a chemical point of view, the composition of the investigated materials is the same as listed in Table 1.

Table 1 Chemical composition of the investigated Ti alloys.

Al%	V%	Fe%	C%	N%	H%	O%	Ti
5.88	3.87	0.14	0.22	0.006	0.002	0.112	Bal.

Finally, for the experimental bulge tests, circular samples with a diameter of 75mm were used; the BULK and the HIPed material had a thickness of 1 mm and 1.5 mm, respectively.

Methods

Experimental tests

Experimental bulge tests were carried out by means of a proper equipped OMCN P30/W press machine. The overview of the experimental setup is provided in Fig. 1a. During bulge tests, the two different layers, placed as schematized in Fig. 1b and clamped by means of a blank-holder pressure of 10MPa , were simultaneously freely deformed into a cylindrical die (diameter and entry fillet radius equal respectively to 45mm and 3mm) heated by means of an induction system managed by a PID controller. The Dome Height (DH) and the temperature were continuously acquired using respectively an optoNCDT 1420 laser sensor and a K-type thermocouple (TC) directly welded on the periphery of the die (Fig. 1b).

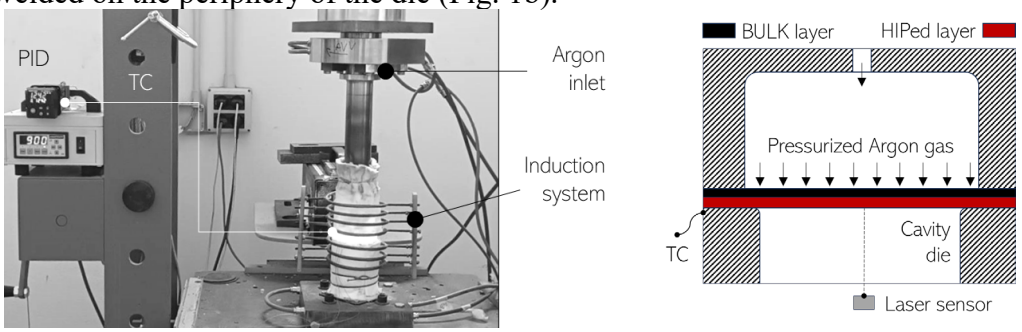

(a) (b)

Fig. 1 experimental setup: (a) overview and (b) scheme of the forming chamber.

The effect of the initial porosity level was investigated in the first part of the experimental campaign. To do this, SSF tests were conducted on the HIPed material for 60 minutes at 850 °C using a furnace (Nabertherm N 61/H); the bulge tests were, thus, performed at 850 °C on both SSFed and HIPed samples.

In the second experimental step, instead of porosity, the effect of the temperature was evaluated by setting an additional temperature level (900 °C) to the previous one and focusing only on the condition after HIP process. Furthermore, as it is preparatory to the subsequent IA, in addition to the experimental curve related to the bilayer, it was necessary to determine the material constants; to do this, the analytical approach by Enikeev and Kruglov [6] was used to determine the BULK material constants. When the temperature was set to 850 °C, an extensive characterization was carried out in a previous work [9]; at 900 °C at least two tests were needed to calculate the material constants of the following power law model.

$$\sigma = C\dot{\varepsilon}^{m} \tag{1}$$

where $\dot{\varepsilon}$ is strain rate, C is a material constant and m represent the strain rate sensitivity index. This last parameter is of fundamental importance; in fact, the higher its value the more superplastic is the material. In Table 2 the experimental tests and the nomenclature adopted for each condition (repeated three times) are summarized.

Table 2 Experimental plan adopted.

Temperature, °C	Pressure, MPa	Type of Sheet	SSF duration, min	Nomenclature adopted
850	1.4	Bilayer	-	HIP_1.4_850
850	1.4	Bilayer	60	60SSF_1.4_850
900	1.4	Bilayer	-	HIP_1.4_900
900	0.56	Bulk	-	BULK_0.56_900
900	1.12	Bulk	-	BULK_1.12_900

As previously mentioned, the analyses related to these experimental tests were based on measurements of both DH over time and thickness after forming along the diametral direction. In this regard, for the measurements of the dome height data from laser sensor were considered; instead, the thickness distributions were obtained by means of a Mitutoyo digital caliper.

Metallographic analyses

Diametral sections of each sample (both after SSF and bulge tests) were properly prepared by grinding and polishing to analyse their porosity. More in detail, the investigation aimed at determining both the average diameter and the percentage area of the porosities according to the different conditions reported in Table 2. For this purpose, the Nikon MA200 microscope and the ImageJ software for digital image processing were adopted respectively to acquire and process the micrographs.

Inverse Analysis

The inverse determination of the material constants from the Backofen's constitutive equation was treated as an optimization problem in which the objective error function, calculated as the difference between the numerical and experimental dome height curve, had to be minimized. Therefore, a simple FE model was created according to a 2D axisymmetric approach (see Fig. 2) by modelling the two blanks as shell deformable bodies whereas keeping the die as a rigid body. Both the blanks were constrained in their outer nodes to simulate the action of the blankholder (not modelled to reduce the computational costs). A constant pressure of 1.4 MPa was applied on the top surface of the bulk blank (reproducing the loading condition of the experimental tests).

The FE model was integrated into an automatic optimization procedure managed by a multi-objective genetic algorithm (MOGA-II): basically, the genetic algorithm (GA) started from an initial population of designs (where the term "design" refers to a single numerical run) and iteratively changed the unknown parameters (the constants of the HIP material) with the final goal of minimizing the error function, expressed by Equation 2 (a more detailed description of the GA-based inverse approach can be found in [10]).

$$ERR = \sum_{i=0}^{N} \left(h_{i,num} - h_{i,exp}\right)^2 \quad (2)$$

Where $h_{i,num}$ refers to the dome height computed by the numerical simulation and $h_{i,exp}$ to the value measured during the test at the same *i*-th instant of time. The optimization procedure was carried out to determine the HIP material's constants at the two investigated levels of temperature according to the experimental plan proposed and discussed in section 2.2.1.

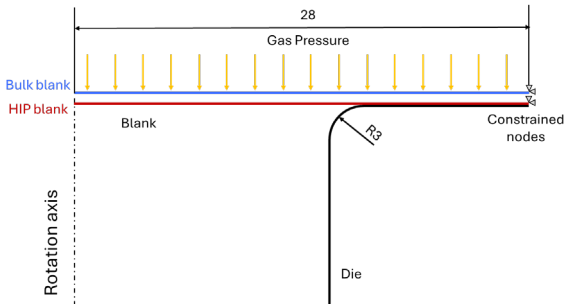

Fig. 2 Scheme of the 2D axisymmetric FE model adopted for the inverse analysis (dimension are in mm).

Process design of the case study

The replacement of a partially damaged mandibular bone was chosen as a case study: once reconstructed the mandibular bone from the DICOM files, the region to be healed was isolated and the geometry of the prosthesis designed starting from mirroring the healthy bone from the opposite side. The final CAD geometry of the implant was used as the base for the definition of the die cavity for the manufacturing process. The sequence of steps is summarized in Fig. 3.

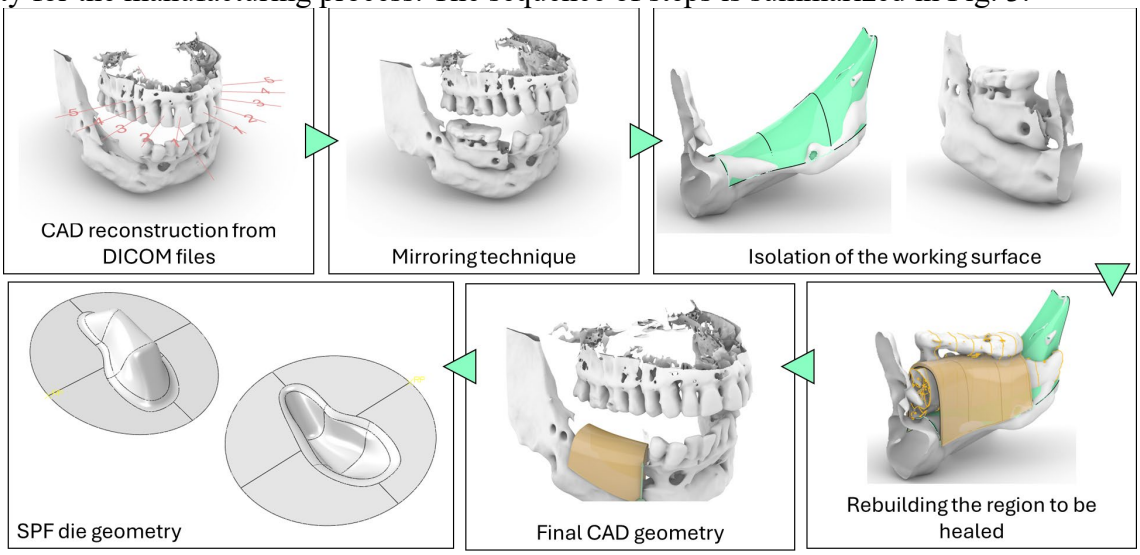

Fig. 3 Definition of the SPF die geometry starting from the DICOM acquisitions.

The created SPF die geometry was implemented in a second FE model to design the SPF process of the case study. An overview of the modelled system is reported in Fig. 4. The two blanks were modelled as 3D shell deformable bodies (meshed by plane-stress elements with an average size of 0.5 mm), whereas the blank as a 3D discrete rigid body (discretized by 1 mm elements on average). Both the blanks periphery was pinned to simulate the action of the blankholder: a constant gas pressure of 1.4 MPa was applied on the top surface of the bulk blank.

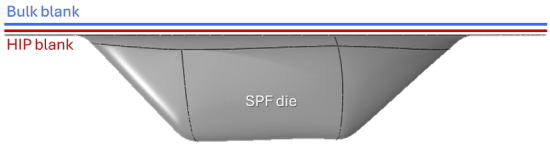

Fig. 4 FE model for the process design of the case study.

Materials Research Proceedings 41 (2024) 1038-1047 https://doi.org/10.21741/9781644903131-114

Results and Discussion

Experimental tests

Results from bulge tests at a constant temperature of 850 °C, in terms of both the Dome Height profile and the thickness distribution, are reported in Fig. 5. These tests were stopped at a final DH of 14 mm.

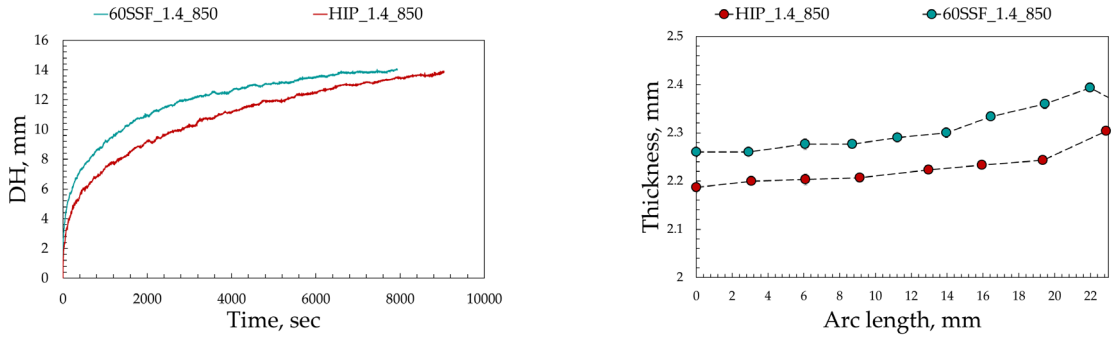

Fig. 5 Experimental results obtained at 850 °C: (a) DH vs Time and (b) Thickness distribution after forming.

It can be observed that a prior SSF of the HIPed material allows a faster increase of DH in the first part of the test; however, keeping the sample at a high temperature during the forming test activates foaming in the sample obtained by HIP. This motivates a gradually decreasing gap between the two conditions tested (Fig. 5a). In particular, the steady-state condition (characterized by a constant slope of the curve) appears to be about very similar for all conditions, suggesting a low effect of pre-foaming on the overall duration of the SPF process. At the same time, SSF allows for an increase in terms of thickness distribution, as demonstrated by the graph in Fig. 5b. This behavior, as better documented by the subsequent metallographic investigations (section 3.2), is due to a higher porosity attributable to the SSFed material.

Fig. 6a, on the other hand, shows the results for the tests conducted at 900 °C; as well as comparisons with what was obtained at 850 °C for the HIPed material are showed in Fig. 6b.

As mentioned in the methodological section, at 900 °C it was also necessary to conduct tests on the BULK material alone to determine in accordance with [6] the material constants (C and m). For this reason, the two tests on BULK were conducted at pressures such that a curve above (red) and below (green) that for the bilayer were obtained (Fig. 6a). The comparison between the two bilayers (Fig. 6b), in addition, shows a clear difference between the two investigated temperatures; despite the fact that the final heights of the two tests are not the same, a temperature increase of 50 ºC allowed a DH value of 14 mm to be reached in 1300 sec rather than 9000 sec, recording a reduction in time of about 590 %.This result surely of remarkable importance for an industrial implementation. Furthermore, as concerns the BULK material, the obtained values of C (2396.65 $MPa \cdot s^{-m}$) and m-value (0.711) show a high propensity to superplasticity of the material in the above described pressure and temperature conditions.

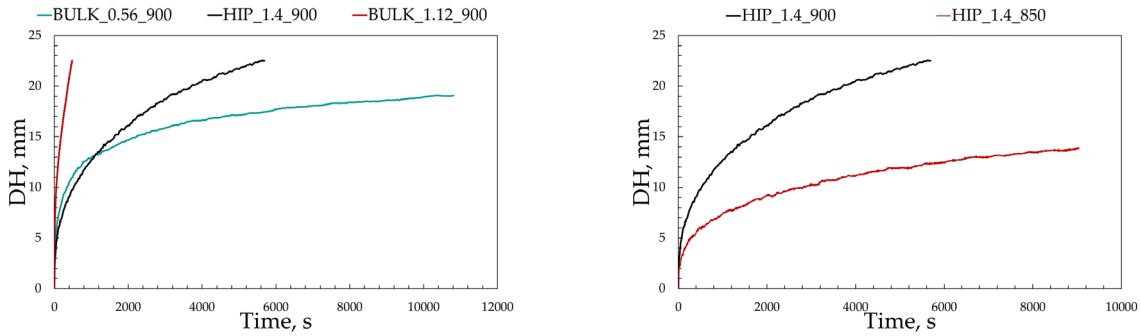

(a) (b)

Fig. 6 DH vs time referred to the HIPed and the BULK conditions at 900 °C (a); effect of the temperature (b)

Metallographic analyses

SSF allowed to increase the porosity (in terms of both average diameter and percentage area) respect to the HIPed material. Marked differences can be found because of the SSF process. In fact, considering an initial average diameter (after HIP process) of only 0.91±0.05 µm, foaming allowed to increase this value up to 14.56±1.50 µm. At the same time, the percentage area changes from 0.65±0.10 % to 4.11±0.60 %. After bulge tests such differences are much smaller.

Beside this, considering the graphs shown in Fig. 7, it is also possible to observe how the level of porosity is strongly influenced by the deformation level (expressed in thinning) reached. The lowest level is referred to the flanged area; the highest is representative of the dome apex.

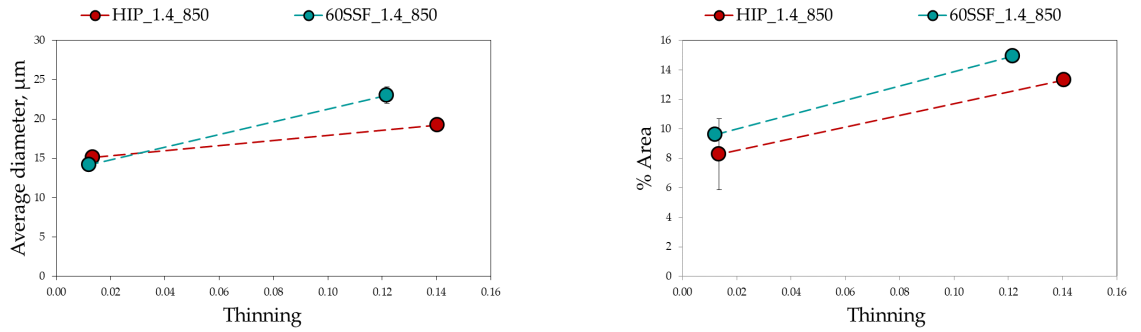

(a) (b)

Fig. 7 Average diameter (a) and percentage area (b) of the porosity after bulge tests at 850 °C according to different thinning levels.

In the flanged area it is particularly evident that the effect of SSF before deformation is somewhat mitigated by the duration of the subsequent bulge test. All these considerations find support from the micrographs summarized in Fig. 8. The black areas are representative of the porosity.

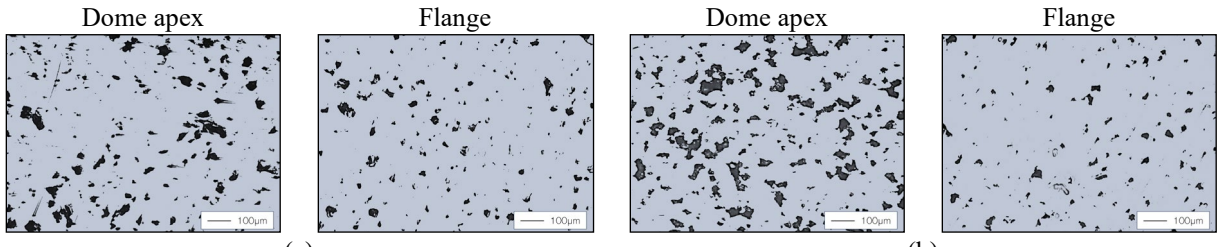

(a) (b)

Fig. 8 Porosity after bulge tests at 850 °C: (a) HIP_1.4_850 and (b) 60SSF_1.4_850.

In light of the obtained experimental results, it is possible to say that the strategy based on SSF prior forming step appears to be not effective, since the effects of the SSF are drastically mitigated by the forming process itself.

On the contrary, regarding the increase in forming temperature (from 850 °C to 900 °C), the effect is also markedly different in terms of porosity. Once again, when considering the porosities as a function of the measured thinning and thus with reference to the two opposite zones (flange and dome apex), it is evident that the two investigated temperatures combined with markedly different forming times lead to varying levels of porosity.

This is supported by both the graphs in Fig. 9. and the micrographs in Fig. 10.

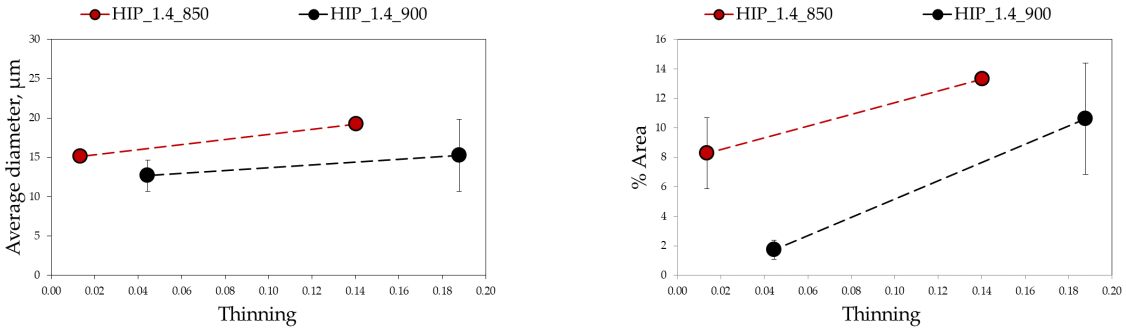

Fig. 9 Average diameter (a) and percentage area (b) of the porosity after bulge tests at different temperature according to different thinning levels.

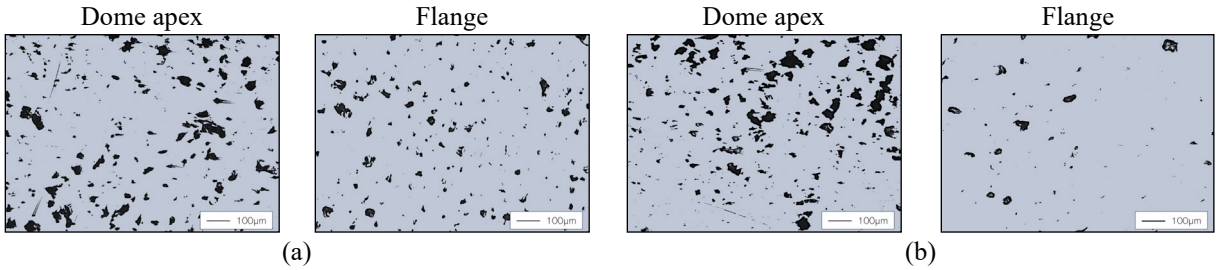

Fig. 10 Porosity after bulge tests at different temperature: (a) HIP_1.4_850 and (b) HIP_1.4_900.

Inverse Analysis

The optimization, for both the investigated levels of temperature, evolved throughout 20 generations (each of 50 individuals). Plotting the results by means of the history charts was an effective way to evaluate the convergence of the GA.

The history charts suggest that the inverse determination of the material constants at 850°C faced some convergence issues (see Fig. 11 a and b): in fact, after approximately 800 designs, the GA tended to stabilize around lower values of both the constants. Different results were recorded for the calibration of the constants at 900°C for which (as visible in Fig. 11 c and d), the convergence was more stable.

Eventually, at the end of each procedure, the best designs could be identified as those characterized by the optimal values of the two material constants able to minimize the error function (their values are resumed in Table 3).

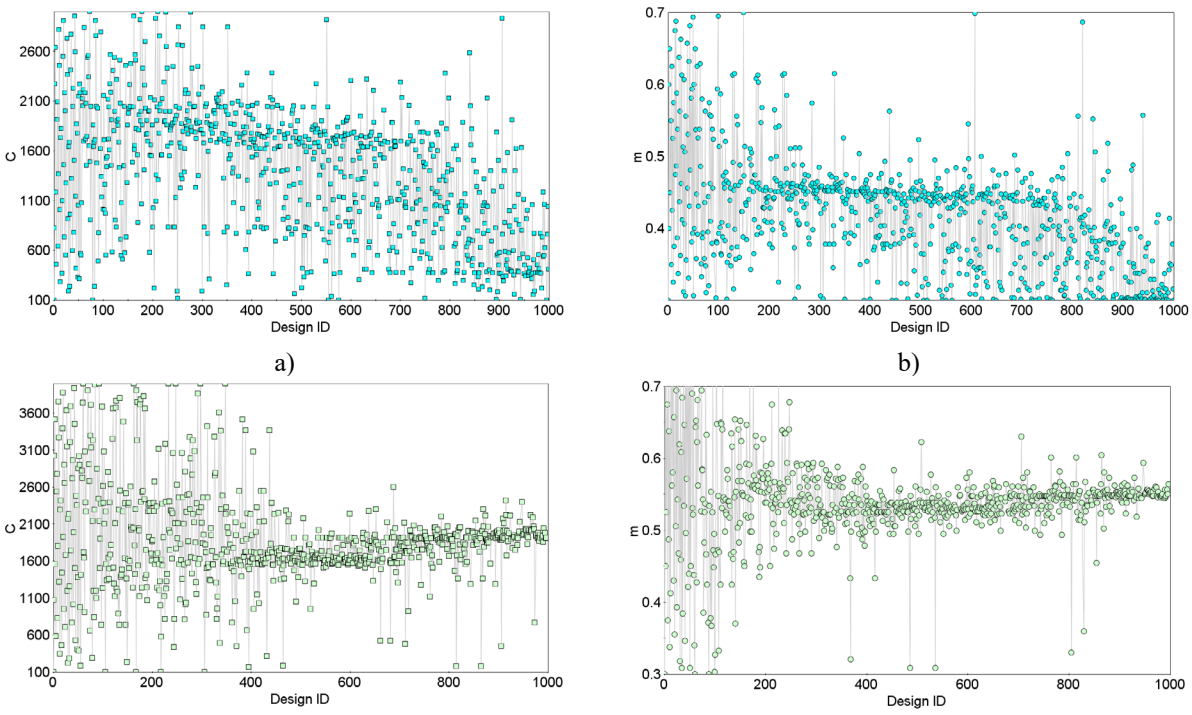

Fig. 11 History charts plotting the evolution of the two parameters throughout the optimization: a) C and b) m at 850°C; c) C and d) m at 900°C.

Table 3 Results from the inverse analysis.

Nomenclature adopted	Temperature, °C	C, MPa·s^m	m
HIP_1.4_850	850	374	0.3
HIP_1.4_900	900	2067.5	0.557

FE simulation of the bilayer implant manufacturing

Results from FE simulations were primarily analysed in terms of die cavity filling with time. Fig. 12 shows the distribution of the COPEN variable which basically represents the clearance between surfaces in contact: more in details, regions of the HIP blank highlighted in blue are in contact with the die surface.

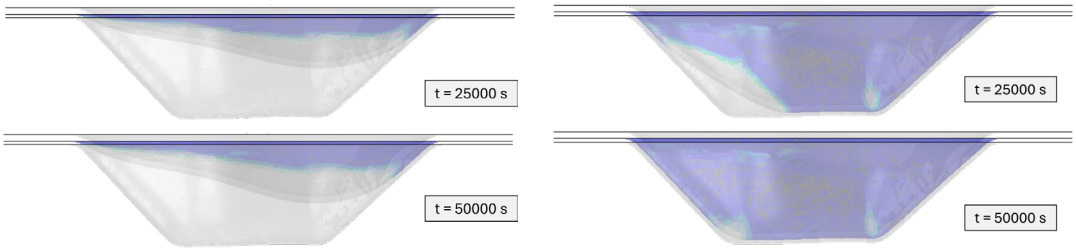

Fig. 12 Filling of the die cavity during the SPF process: a) T=850°C, b) T=900°C

It could be then concluded that, at 850°C and even after 50000 s, the bilayer blank was not in contact with the bottom part of the die. On the other hand, when raising the temperature at 900°C, the blank got in contact with the bottom of the die cavity already after 25000 s. The different filling at the two investigated temperatures is coherent with the results from the material characterization (see Fig. 6b) and led to the conclusion that rising the temperature up to 900°C could be an effective way to obtain the final geometry without excessively prolonging the manufacturing time.

Conclusions

In the present work, based on experimental tests, the effect of both initial level of the porosity and the temperature were investigated in order to numerically design a hybrid full custom prosthesis made from a Ti bilayer having one layer derived from HIP process and one monolithic layer. Main outcomes of the investigation are summarized below:

- The initial level of porosity seems to be less effective on the superplastic behavior of the HIPed layer, as the SPF conditions mitigated the effect of the previous SSF.
- Increasing the SPF temperature, on the other hand, makes it possible to significantly reduce the production time while still ensuring that the deformation behavior of the material is maintained, as supported by the high m-value which was determined.
- The IA showed a better capability to determine material constants at 900 °C; moreover, the obtained values of C and m suggest an emphasized propensity of the material to exhibit superplastic properties at 900 °C.
- The numerical design of the SPF process for the manufacturing of a full custom prosthesis has confirmed that the adoption of higher process temperature (900 ºC) allows a drastic reduction in process time (while at 900 °C the prosthesis is formed after about 50000 seconds, at 850 °C, after the same time, the bilayer did not fully touch the die).

References

[1] M.W. Kearns, Formation of Porous Bodies, 1987.

[2] S. Oppenheimer, D.C. Dunand, Solid-state foaming of Ti-6A1-4V by creep or superplastic expansion of argon-filled pores, Acta Mater 58 (2010) 4387–4397. https://doi.org/10.1016/j.actamat.2010.04.034.

[3] P. Guglielmi, A. Piccininni, A. Cusanno, A.A. Kaya, G. Palumbo, Mechanical and microstructural evaluation of solid-state foamed Ti6Al4V-ELI alloy, Procedia CIRP 110 (2022) 105–110. https://doi.org/10.1016/j.procir.2022.06.021.

[4] P. Guglielmi, A. Cusanno, I. Bagudanch, G. Centeno, I. Ferrer, M.L. Garcia-romeu, Experimental and numerical analysis of innovative processes for producing a resorbable cheekbone prosthesis, J Manuf Process 70 (2021) 1–14. https://doi.org/10.1016/j.jmapro.2021.07.060.

[5] D. Sorgente, L. Tricarico, The role of the numerical simulation in superplastic forming process analysis and optimization, Key Eng Mater 433 (2010) 225–234. https://doi.org/10.4028/www.scientific.net/KEM.433.225.

[6] F.U. Enikeev, A.A. Kruglov, An analysis of the superplastic forming of a thin circular diaphragm, Int J Mech Sci 37 (1995) 473–483. https://doi.org/10.1016/0020-7403(94)00081-T.

[7] D. Sorgente, G. Palumbo, A. Piccininni, P. Guglielmi, L. Tricarico, Modelling the superplastic behaviour of the Ti6Al4V-ELI by means of a numerical/experimental approach, International Journal of Advanced Manufacturing Technology 90 (2017) 1–10. https://doi.org/10.1007/s00170-016-9235-7.

[8] P. Guglielmi, A. Piccininni, A. Cusanno, G. Paumbo, Manufacturing of a hybrid component in Ti6Al4V-ELI alloy by combining diffusion bonding and superplastic forming, in: Materials Research Proceedings, Association of American Publishers, 2023: pp. 37–44. https://doi.org/10.21741/9781644902714-5.

[9] D. Sorgente, G. Palumbo, A. Piccininni, P. Guglielmi, S. Aksenov, Investigation on the thickness distribution of highly customized titanium biomedical implants manufactured by superplastic forming, CIRP J Manuf Sci Technol Accepted, (2017).

[10] A. Piccininni, D. Sorgente, G. Palumbo, Genetic Algorithm based inverse analysis for the superplastic characterization of a Ti-6Al-4V biomedical grade, Finite Elements in Analysis and Design 148 (2018) 27–37.